Aromatic aldehydes as tuneable and ppm level potent promoters for zeolite catalysed methanol dehydration to DME

Zhiqiang Yang,[a] Benjamin J. Dennis-Smither,*[b] Corneliu Buda,[c] Amie Easey,[b] Fiona Jackson,[b] Gregory A. Price,[b] Neil Sainty,[b] Xingzhi Tan,[a] Zhuoran Xu,[c] and Glenn J. Sunley*[b]

Dimethyl ether (DME) is a valuable chemical intermediate and renewable fuel that can be made, via methanol, from many sources of carbon, including carbon dioxide and biomass. Benzaldehyde and its derivatives have been found to be promoters for zeolite catalysed methanol dehydration to DME at low temperature (110 to 150 °C). For the 3-dimensional medium pore zeolite H-ZSM-5 (MFI) the promotion is readily reversible and the potency of the promoter can be tuned by varying the substituent on the aromatic ring of the aldehyde. The most potent promoters are active at concentrations as low as 1 ppm relative to methanol. High throughput experimentation (HTE) is used to screen and rank potential promoters and catalysts and to collect high quality kinetic data for the most promising candidates discovered. The catalytic data and *in-situ* FT-IR-MS experiments combined with molecular modelling studies indicate a mechanism involving competitive adsorption of the aldehyde promoter on a Brønsted acid (BA) site, followed by reaction with methanol to give a hemi-acetal intermediate. Loss of water from the hemi-acetal intermediate generates a transient and highly reactive methyl oxonium species, $[ArC(H)(=O\text{-}Me)]^+$, which then directly reacts with methanol via a S_N2 mechanism to give DME and regenerate the aldehyde promoter and BA site. The methyl oxonium species is stabilized by electron-donating groups on the aromatic ring and the solvent like effect of the zeolite pore walls. Molecular descriptors were calculated by molecular modelling for the 22 aromatic aldehyde promoters tested. Multivariate linear regression analysis was used to build an interpretable model for aldehyde promotional activity in H-ZSM-5 and in another 3-dimensional medium pore zeolite, H-ZSM-11 (MEL).

Introduction

The tuning of the properties and activity of aromatic compounds by ring substitution is one of the most widely applied concepts in chemistry. It has wide relevance and applicability in organic chemistry and many biological systems.[1] In homogeneous catalysis with metallo-organic and organometallic complexes aromatic ring substitution is used to tune catalyst performance via both bonded and non-bonded interactions, for example in ethylene oligomerisation and polymerisation, olefin metathesis, carbonylation, and various coupling reactions used in organic synthesis.[2-7] Zeolites are an important class of heterogeneous catalysts widely utilized in industry. The solvent-like confinement effect of the zeolite micropores stabilizes intermediates and lowers the energy of transition states in key reaction steps.[8] Organo-catalysis by guest species in the zeolite pores is a promising area for exploration and offers the potential to fine-tune the catalytic properties of zeolites.[9] We have recently shown that methyl esters can act as potent promoters for zeolite catalysed methanol dehydration to dimethyl ether (DME).[10] Aromatic species, including methylated benzenes, trapped in zeolite pores play a key role in the industrially important methanol to hydrocarbons (MTH) reaction at elevated temperatures (> ca. 250°C), via the well-known hydrocarbon pool mechanism.[11-19] These species also evolve to give recalcitrant polycyclic aromatic residues, resulting in severe catalyst deactivation.[19] In contrast at lower reaction temperatures (110 to 150 °C) we find that aromatic compounds with a functional group, such as a formyl group, can result in unexpected and highly selective chemistry, which is enhanced by the zeolite confinement effect.

DME is a valuable chemical intermediate and renewable fuel that can be made, via methanol, from many sources of carbon, including from carbon dioxide, municipal solid waste, biogas and biomass.[20, 21] In this paper we demonstrate the reversible promotion of zeolite catalysed methanol dehydration to DME (M2D) by benzaldehyde and its derivatives.[22] The aromatic aldehyde promoters can be tuned by varying the substituents on the aromatic ring and can show significant activity down to concentrations as low as 1 part per million (ppm) relative to methanol. High throughput experimentation (HTE) is used to screen and rank potential promoters and catalysts and to collect high quality kinetic data for the most promising candidates discovered. The promoter ranking and kinetic data is combined with *in-situ* Fourier transform infra-red mass spectrometry (FT-IR-MS) experiments, molecular modelling and multivariate linear regression analysis to build a mechanistic description of how the aromatic aldehyde promoters function and the key factors that influence their potency.

Experimental

Catalyst and promoter testing

The methanol dehydration reactions were carried out using a 16-channel parallel fixed-bed reactor Flowrence™ system from Avantium NV, using stainless steel reactors of 2 mm internal diameter with a length of 300 mm. The liquid feed was introduced by a HPLC pump into a heated zone (220 ^oC) along with inert gas feeds before feeding to the reactors. In a typical experiment fifteen of the reactors were packed with 25 ±0.5 mg of catalyst, having a particle size fraction of 100 to 200 µm diameter. The effluent stream from each reactor was diluted with inert gas (nitrogen) and was periodically analysed by online gas chromatography (GC) to determine the yield of DME product. Space time yields (STY) in grammes per kilogramme of catalyst per hour (g kg^{-1} h^{-1}) for making DME from methanol were determined between 18 and 24 hours after introducing the methanol only feed. Space time yields for making DME from methanol in the presence of an additional organic component were typically determined between 1 and 24 hours after introducing the organic additive. Further details of the catalyst testing protocol and catalysts and reagents used are given in the ESI.

Dew point calculations were performed to ensure that all the aldehyde promoters were tested at partial pressures such that they remained in the vapour phase at the reactor inlet. Some of the promoters tested in this work are very potent and promote methanol dehydration to DME at concentrations as low as 0.0001 mol % (1 ppm) relative to methanol fed. It is therefore important to flush the process lines with clean methanol for at least 24 hours at the end of each experiment to remove any traces of the promoter from the testing equipment. In addition, the standard testing protocol used fresh and clean methanol at the start of each experiment, to ensure that the baseline conditions had been returned to before subsequently testing a promoter diluted in methanol.

***In-situ* FT-IR-MS studies**

Fourier transform infra-red (FT-IR) spectra were collected using a high temperature reaction cell from Harrick Scientific. The reaction cell was equipped with ZnSe windows, with the reaction cell operated at ambient pressure. FT-IR spectra were collected with a Thermo Scientific™ Nicolet™ iS50 spectrometer equipped with an MCT detector and KBr beam-splitter and were measured in the transmission mode. The reactant under study was then introduced into the reaction cell by sparging nitrogen through the liquid reactant placed in a saturator operated at room temperature. The gaseous effluent from the reaction cell was sampled with a capillary connected to a Dycor mass spectrometer (Ametek), with the evolution of DME from the zeolite sample being determined by monitoring the m/z signal at 46. Experimental details are given in the ESI.

Ammonia temperature programme desorption

Ammonia temperature programmed desorption (TPD) analysis of some of the catalysts tested was carried out using a fully automated Altamira AMI-200 Chemisorption Analyser. Full details are given in the ESI.

Molecular modelling studies

The methodology used for the calculation of the energies of reaction intermediates and transition states and adsorption energies of the aromatic aldehydes in H-ZSM-5 was the same as that used in a previous publication.[10] Further details are given in the ESI. H-ZSM-5 molecular modelling simulations used 288 framework atoms, compromised of 95 Si and 192 O atoms, with one of the T-atoms in the framework substituted with an Al atom to create a Brønsted acid (BA) site. For the molecular modelling work a representative BA site was selected at the intersection of the straight and sinusoidal channels, selecting the O2 site located between the T1 and T2 sites with the T1 site selected for the Al location. The adsorption, reaction intermediate and transition state energies reported here are associated with enthalpy contributions, without any temperature corrections applied. Information on the methods used to calculate the molecular descriptors for the 22 aromatic aldehydes tested is given in the ESI.

Data analysis and multivariate linear regression analysis

Data analysis was performed using JMP® software from JMP Statistical Discovery LLC. The forward stepwise regression feature in JMP was used to build models with DME space time yield data and normalised descriptors for benzaldehyde and mono-substituted benzaldehydes and the models were analysed using standard metrics (RMSE and R^2). Further details for data analysis and multivariate linear regression (MLR) modelling are given elsewhere in the paper and in the ESI.

Results and discussion

Promoter and catalyst testing

As in our previous studies[10] we chose to investigate the impact of organic additives on the M2D reaction at 150 ^oC and a methanol partial pressure of 110 kPa. These relatively mild conditions allow MTH chemistry to be avoided, with a high reaction selectivity to DME (> 99%). Under these conditions the M2D reaction is zero order in methanol, indicating high active site coverage. These are realistic conditions for studying competitive adsorption effects relevant to the presence of low level impurities in industrial processes. The impact on DME STY of co-feeding benzaldehyde, 0.1 mol % relative to methanol, was evaluated for four 3-dimensional zeolites, Fig. 1.

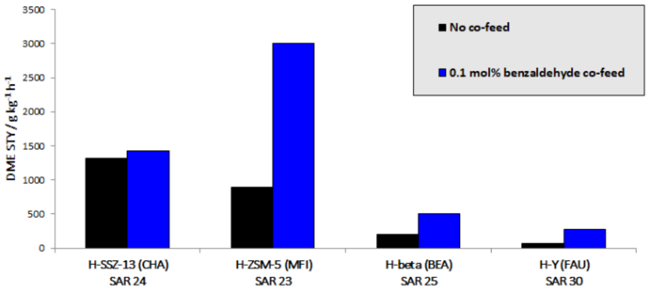

Fig. 1 Impact of co-feeding benzaldehyde on DME STY for four different zeolites. SAR = silica-alumina ratio, letters in brackets zeolite framework code. Conditions: 150 °C, methanol WHSV 17.1 h^{-1}, methanol partial pressure 110 kPa, benzaldehyde partial pressure 0.11 kPa.

For the narrow pore zeolite H-SZZ-13 (CHA) only a small increase (ca. 10 %) in DME STY was observed. Much more significant increases in DME STY were observed for the medium pore zeolite H-ZSM-5 (MFI) and the wide pore zeolites H-beta (BEA) and H-Y (FAU). The wide pore zeolites however showed signs of deactivation in the presence of benzaldehyde. In contrast the medium pore zeolite showed good stability, a high DME STY and returned to its original activity with methanol only when the benzaldehyde was removed from the methanol feed, Fig. 2.

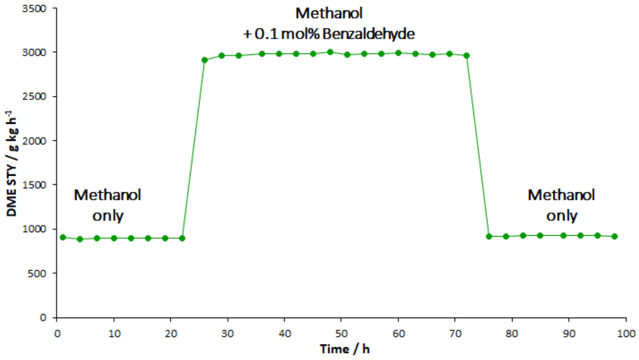

Fig. 2 Impact of co-feeding benzaldehyde on DME STY for H-ZSM-5 SAR 23. Conditions: 150 °C, methanol WHSV 17.1 h^{-1}, methanol partial pressure 110 kPa, benzaldehyde partial pressure 0.11 kPa.

H-ZSM-5 was thus selected for a more detailed study. H-ZSM-5 with a silica to alumina (SAR) of 23, 80 and 280 was tested at 150 °C, under the same conditions as described above. Significant promotion of DME STY was seen for all the H-ZSM-5 catalysts, Fig. 3.

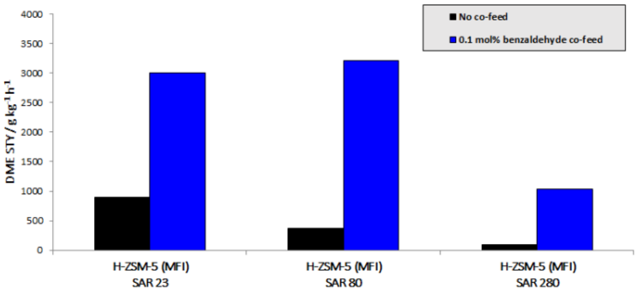

Fig. 3 Impact of co-feeding benzaldehyde on DME STY for H-ZSM-5 SAR 23, SAR 80 and 280. Conditions: 150 °C, methanol WHSV 17.1 h^{-1}, methanol partial pressure 110 kPa, benzaldehyde partial pressure 0.11 kPa.

Larger promotions were seen for the higher SAR materials, SAR 280 (11) > SAR 80 (9) > SAR 23 (3), promotional factors in parentheses, expressed as the ratio of the DME STY for the promoted versus unpromoted reaction. As a result of this promotional behaviour the SAR 80 catalyst gave a higher DME STY, of 3215 g kg^{-1} h^{-1}, than the SAR 23 catalyst, which gave a

DME STY of 3000 g kg^{-1} h^{-1}. The SAR 280 catalyst gave a DME STY of 1036 g kg^{-1} h^{-1}. The larger promotion with the higher SAR materials may be related to the increased hydrophilicity of low SAR zeolites[23] when used in the promoted M2D reaction described here, with the water co-product acting as an inhibitor of promotion. Indeed addition of water (5 mol %) reduced the DME STY for the H-ZSM-5 SAR 80 catalyst from 559 to 149 g kg^{-1} h^{-1} when tested with 5 mol % benzaldehyde in the methanol feed at 110 ^{o}C. The methanol only reaction under these conditions gave a DME STY of 16 g kg^{-1} h^{-1}, indicating that although water inhibits promotion the benzaldehyde promoter can still effectively function in the presence of water.

In the H-ZSM-5 M2D experiments with benzaldehyde the promoter passed over the catalysts essentially unconverted, with only trace amounts of benzaldehyde dimethyl acetal (BDA) being detected in the reactor effluent when 1 mol % benzaldehyde was tested at 150 ^{o}C; see Fig. S2 in the ESI. The presence of BDA in the reaction effluent was more apparent at lower reaction temperatures, where its formation is thermodynamically more favourable and there is less water available from the M2D reaction for its hydrolysis; see ESI Fig S3 for representative GC traces. Its concentration was however still very low compared to the aldehyde. BDA, added at 1 mol %, was also tested at 150 ^{o}C as a promoter with H-ZSM-5 SAR 80. The presence of BDA increased the DME STY from 388 to 6860 g kg^{-1} h^{-1}; benzaldehyde tested under these conditions gave a very similar DME STY, 6590 g kg^{-1} h^{-1}. The BDA was almost fully hydrolysed to benzaldehyde under these conditions and GC traces of the reactor effluents from reactions promoted with BDA and benzaldehyde were essentially identical. This indicates facile interconversion of benzaldehyde and BDA under the reaction conditions reported here (110 to 150 ^{o}C) for the M2D reaction. H-ZSM-5 is reported to be an effective catalyst for the synthesis of BDA from benzaldehyde and methanol at ambient temperature.[24] In a control experiment toluene, tested at 0.1 mol % and 150 ^{o}C, had no discernible impact on the H-ZSM-5 catalysts, in contrast to the behaviour of toluene in MTH chemistry at higher temperature.[12] This illustrates the importance of the formyl functional group on promoter activity.

H-ZSM-5 SAR 80 was selected to be tested for the M2D reaction with a range of benzaldehyde derivatives at 150 ^{o}C, using 0.01 mol % of benzaldehyde as the reference point, Fig. 4. This kept the methanol conversion for the reference point well below 10%, to allow for a sensible range of conversion for the ranking of the aldehyde promoters. Under these conditions the DME STY for the unpromoted reaction was 388 g kg^{-1} h^{-1}.

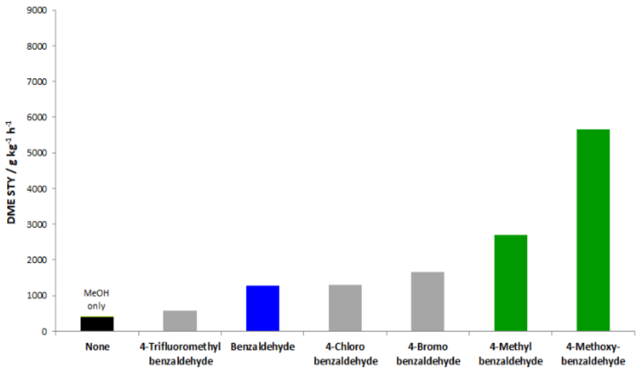

Fig. 4 Impact of co-feeding benzaldehyde derivatives on DME STY for H-ZSM-5 SAR 80. Conditions: 150 ^{o}C, methanol WHSV 17.1 h^{-1}, methanol partial pressure 110 kPa, aldehyde partial pressure 0.011 kPa. Black bar methanol only, blue bar benzaldehyde, green bars electron-donating substituents and grey bars electron-withdrawing substituents

In Fig. 4 the impact on DME STY of substituting a range of electron-donating and -withdrawing groups on the 4-position of the aromatic ring was assessed. All the aldehydes promoted the M2D reaction, with electron-donating groups, 4-Me and 4-OMe, giving the largest increases in DME STY. The aldehyde promoter with strongly electron-withdrawing 4-CF_3 group gave the smallest increase in DME STY. Benzaldehyde derivatives with moderately electron-withdrawing groups either gave a DME STY comparable to benzaldehyde, for 4-chloro-benzaldehyde, or somewhat surprisingly for 4-bromobenzaldehyde ahigher DME STY than benzaldehyde. Under the same conditions as tested in Fig. 4 introduction of a methyl group into the sterically hindered 2-position gave a DME STY of 841 g kg^{-1} h^{-1} for 2-methylbenzaldehyde, compared to DME STY's of 1965 and 2709 g kg^{-1} h^{-1}, for 3-methylbenzaldehyde and 4-methylbenzaldehyde respectively.

We have previously shown that the potency of aliphatic methyl esters, RCO_2Me, as promoters for the M2D reaction can be markedly enhanced by increasing the length of the alkyl chain R, which more firmly anchors the promoters in the zeolite pores via non-bonded van der Waals forces.[10] The impact on DME STY of the length of the alkyl chain in the 4-position of benzaldehyde was therefore assessed, see Fig. 5. Increasing the length of the alkyl chain increases the potency of the promoter, with 0.01 mol % 4-n-pentylbenzaldehyde being particularly potent, giving a DME STY of 7815 g kg^{-1} h^{-1}, representing a 20-fold increase in DME STY under these conditions.

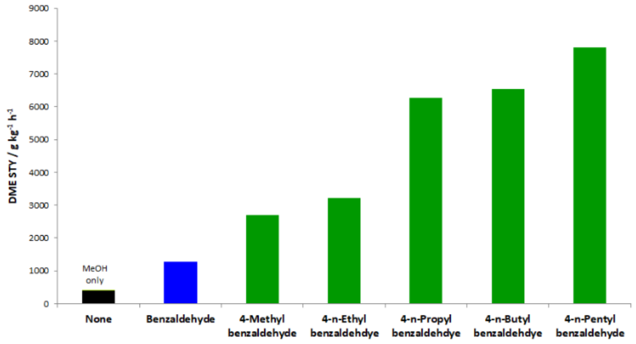

Fig. 5 Impact of co-feeding benzaldehyde and 4-alkylbenzaldehydes on DME STY for H-ZSM-5 SAR 80. Conditions: as in Fig. 4. Black bar methanol only.

In total, in addition to benzaldehyde, 21 benzaldehyde derivatives were tested at 150 °C for promotion of the M2D reaction with H-ZSM-5 SAR 80 and another 3-dimensional medium pore zeolite, H-ZSM-11 (MEL) SAR 50. Most of these promoters were also tested at 110 °C with H-ZSM-5 SAR 80. The data for these experiments is given in Tables S2 and S3 in the ESI. The 4-n-pentylbenzaldehyde promoter was also tested at 150 °C with H-ZSM-5 SAR 80 at a reduced methanol WHSV of 4.3 h^{-1}. At a concentration of 0.01 mol % the aldehyde increased the methanol conversion from 12% for the unpromoted reaction to 88% for the promoted reaction. At this high conversion, the M2D reaction remained highly selective to DME (> 99%), with negligible amounts of by-products being formed. This experiment also shows that the promoters are effective over a wide range of methanol conversion, even when considerable amounts of water are being produced by the methanol dehydration reaction.

Kinetic and other data collected at lower temperature

Kinetic data for a selection of the promoters with H-ZSM-5 SAR 80 was collected at 110 °C. At this temperature the methanol conversion for the unpromoted M2D reaction was well below 1%, with a DME STY of 16 g kg^{-1} h^{-1}. Using these conditions, the impact on DME STY of the concentration of the most potent promoter 4-n-pentylbenzaldehyde was evaluated, Fig. 6.

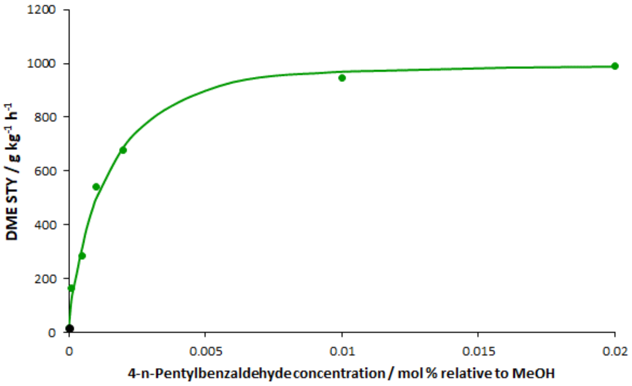

Fig. 6 Impact of co-feeding different concentrations of 4-n-pentylbenzaldehyde derivatives on DME STY for H-ZSM-5 SAR 80. Conditions: 110 °C, methanol WHSV 17.1 h^{-1}, methanol partial pressure 110 kPa, aldehyde partial pressure 0.00011 to 0.022 kPa. Black dot methanol only. Green line added to guide the eye.

With this very potent promoter saturation kinetics were approached at a concentration of 0.02 mol %, with a 62-fold increase in DME STY to 990 g kg^{-1} h^{-1} being observed. Indeed this promoter was so potent that only 0.0001 mol % (1 ppm) of it was required to increase the DME STY by 10-fold to 165 g kg^{-1} h^{-1}. In contrast benzaldehyde required a concentration of 5 mol % to approach saturation kinetics, giving a significantly lower DME STY of 559 g kg^{-1} h^{-1} at these conditions, see Fig. S6 in the ESI. Concentration studies were also performed for 4-Me-benzaldehyde, 4-CF_3-

benzaldehyde, 4-Cl-benzaldehyde and 4-MeO-benzaldehyde. All these promoters approached saturation kinetics at lower concentrations (1 mol % or less) than benzaldehyde, see Fig. S6 and Fig. S7 in the ESI. In these concentration studies the maximum DME STY observed (numbers in parentheses, in g kg^{-1} h^{-1}) for the promoters followed the trend 4-n-pentylbenzaldehyde (990) > 4-MeO-benzaldehyde (925) > 4-Me-benzaldehyde (728) > benzaldehyde (559) > 4-Cl-benzaldehyde (305) > 4-CF$_3$-benzaldehyde (66).

Next the impact of methanol partial pressure on DME STY was evaluated for the 4-n-pentylbenzaldehyde promoted M2D reaction. The concentration and partial pressure of the aldehyde, 0.0005 mol % and 0.00055 kPa, was chosen such it was well away from saturation kinetics at 110 kPa of methanol. The methanol partial pressure was then varied whilst keeping the aldehyde partial pressure constant at 0.00055 kPa, see Fig. S11 in the ESI. Reducing the methanol partial pressure under these conditions increased the DME STY from 287 g kg^{-1} h^{-1} at 110 kPa of methanol to 484 and 652 g kg^{-1} h^{-1} at 55 and 27.5 kPa of methanol respectively. A similar inverse dependence on methanol partial pressure was observed with benzaldehyde, see ESI Fig. S12. The data above is consistent with a promotional mechanism involving competitive adsorption between the aldehyde promoter and methanol on an active site, with the adsorbed aldehyde facilitating an alternative and more facile reaction pathway to make DME from methanol.

The effect of co-feeding water, 5 mol % relative to methanol, on the promoted M2D reaction was explored at 110 °C for H-ZSM-5 SAR 80, tested with 0.01 mol % 4-n-pentylbenzaldehyde (methanol WHSV of 17.1 h^{-1}). The addition of water to the feed was found to reduce the DME STY from 946 to 237 g kg^{-1} h^{-1}. However even with this amount of water added to the feed, equivalent to that formed at 10 % methanol conversion, there was still a 15-fold increase in DME STY versus the methanol only reaction.

The importance of the zeolite micropores in boosting the potency of the aldehyde promoters was explored by comparing H-ZSM-5 SAR 80 with a molecular acid, silicotungstic acid (STA), supported on mesoporous silica. Both catalysts were tested with 0.01 mol % of benzaldehyde and a series of 4-alkyl substituted benzaldehydes, Fig. 7.

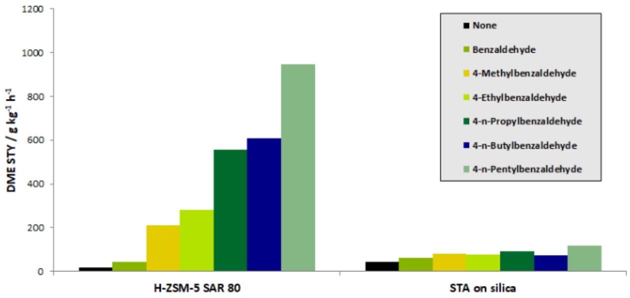

Fig. 7 Impact of co-feeding benzaldehyde and 4-alkylbenzaldehydes on DME STY for H-ZSM-5 SAR 80 and STA on silica. Conditions: 110 °C, methanol WHSV 17.1 h^{-1}, methanol partial pressure 110 kPa, aldehyde partial pressure 0.011 kPa. Black bars methanol only.

As the alkyl group was lengthened from methyl to n-pentyl there was a significant increase in DME STY across the series for the H-ZSM-5 SAR 80 catalyst. The DME STY increased from 16 g kg^{-1} h^{-1} for the unpromoted reaction to 946 g kg^{-1} h^{-1} for the most potent promoter tested, 4-n-pentylbenzaldehyde, a 59-fold increase in DME STY. In contrast beyond 4-methylbenzaldehyde there was no strong effect of alkyl chain length on DME STY for the STA on silica catalyst, with the DME STY increasing from 43 g kg^{-1} h^{-1} for the unpromoted reaction to 116 g kg^{-1} h^{-1} for the 4-n-pentylbenzaldehyde promoted reaction. The Brønsted acid (BA) sites in the H-ZSM-5 SAR catalyst were found on average to be turning over ten times faster (see Fig. S14 in the ESI) for making DME than those in the STA on silica catalyst when tested with 0.01 mol % 4-n-pentylbenzaldehyde, illustrating the significance of the zeolite confinement effect on promoter potency.

Lastly the effectiveness of the 4-pentylbenzaldehyde promoter on the M2D reaction in the presence of added water was compared for H-ZSM-5 SAR 80 versus STA on silica, using the reaction conditions above. For the H-ZSM-5 catalyst, with 5 mol % water in the methanol feed, addition of 0.01 mol % of 4-pentylbenzaldehyde significantly increased the DME STY, from 10 to 237 g mol kg^{-1} h^{-1}, resulting in a 24-fold increase in DME STY. In contrast, for the STA on silica catalyst, with 5 mol % water in the methanol feed, addition of 0.01 mol % of 4-pentylbenzaldehyde only slightly increased the DME STY, from 36 to 44 g mol kg^{-1} h^{-1}, showing only a 1.2 fold increase in DME STY. This suggests that the confines of the zeolite, combined with its high SAR, and structure of the promoter, create a favourable environment[25, 26] for the M2D reaction, even in the presence of excess water.

In-situ FT-IR-MS studies

The interaction of the aldehyde promoters and methanol with H-ZSM-5 was investigated in a high temperature reaction cell by *in-situ* FT-IR spectroscopy coupled with MS analysis of the reactor effluent to monitor the evolution of DME from the zeolite catalyst. At 110 ºC treatment of H-ZSM-5 SAR 23 with flowing N_2 saturated with benzaldehyde vapour resulted in complete titration of the BA sites at 3609 cm^{-1}, Fig. 8.

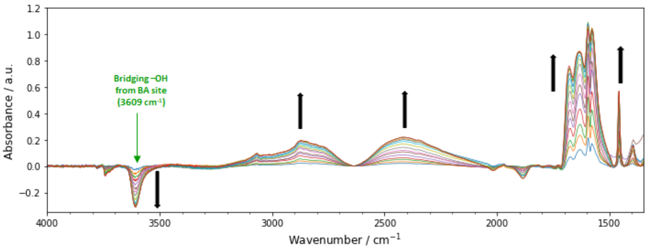

Fig. 8 FT-IR difference spectra for H-ZSM-5 SAR 23 treated with benzaldehyde at 110 ºC. Spectra collected over a period of 15 minutes, at a time interval of 1 per minute. Black arrows show direction with time.

Concurrent with titration of the BA sites a strong IR band appeared at 1578 cm^{-1}, associated with a protonated C=O bond vibration strongly coupled with aromatic ring vibrations. A strong and sharp IR band at 1597 cm^{-1}, associated with aromatic ring vibrations strongly coupled with protonated formyl group vibrations, was also evident.‡ A medium intensity and sharp IR band at 1458 cm^{-1}, associated with aromatic ring vibrations, was also observed. A broad IR band in the ca. 2200 to 2600 cm^{-1} region was also present, indicative of perturbation of BA site O-H bonds via a strong interaction with the aldehyde C=O group. During the benzaldehyde dosing of the zeolite sample a new broad IR band also appeared at ca. 1635 cm^{-1}, characteristic of a C=O group, attached to an aromatic ring, interacting with Al^{3+} Lewis acid (LA) sites.[27, 28] Consistent with adsorption of benzaldehyde on the zeolite IR bands associated with aromatic C-H bond vibrations, 3070 cm^{-1}, and formyl C-H bond vibrations, broad bands in the 2650 to 2900 cm^{-1} region, were also observed.[29] The silanol groups in the zeolite, centred at 3740 cm^{-1},[30] were also titrated, concurrent with the appearance of an IR band at 1680 cm^{-1}, indicative of the C=O group of the aldehyde H-bonded to silanol -OH groups. After exposure to benzaldehyde purging the zeolite sample with N_2 at 110 ºC partially regenerated the silanol groups, indicating a relatively weak interaction between benzaldehyde and at least some of the silanol groups. In contrast the BA sites remained titrated, indicating a strong interaction between benzaldehyde and the BA sites. Similar spectra were obtained for when H-ZSM-5 SAR 80 was exposed to benzaldehyde, see ESI Fig. S16. However, in this case the SAR 80 zeolite sample was richer in silanol groups, resulting in differences in relative IR band intensities in the 1570 to 1700 cm^{-1} region. For the SAR 80 material the broad IR band due to the C=O group interaction with Al^{3+} LA sites (1635 cm^{-1}) was significantly weaker relative to the other bands in this region (1570 to 1700 cm^{-1}) than in the SAR 23 material. This observation suggests that LA sites likely do not play a significant role in benzaldehyde promotion of the M2D reaction, given the stronger promotion observed with the higher SAR catalyst, *vide supra*. A role of the LA sites in promoting the M2D reaction cannot however be entirely excluded, as they have been reported to play a cooperative role with BA sites in the etherification and acetalization of 5-hydroxymethylfurfural with ethanol.[31]

The H-ZSM-5 SAR 23 sample, with its BA sites titrated with benzaldehyde, was exposed to a stream of N_2 saturated with methanol, see time resolved FT-IR spectra in Fig. 9.

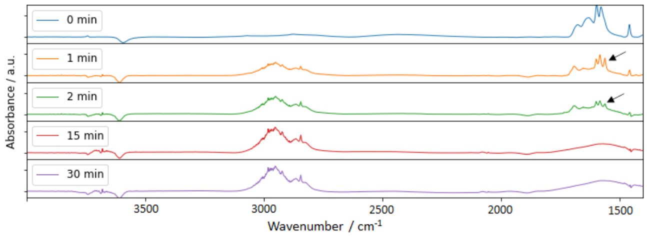

Fig. 9 Time resolved FT-IR difference spectra for H-ZSM-5 SAR 23 titrated with benzaldehyde and purged with N_2 (spectrum at 0 minutes) and then exposed to methanol at 110 ºC. Time intervals as indicated. Black arrows indicate new IR band at 1564 cm^{-1} observed 1 and 2 minutes after exposure to methanol.

After one minute of exposure to methanol a new and distinctive band appeared at 1564 cm^{-1}. Broad IR bands between ca. 2800 and 3100 cm^{-1}, C-H bond vibrations, due to adsorbed methanol species were also observed.[32, 33] As adsorbed DME also has IR bands in this region,[32] it may also be already present at low levels at this stage of the reaction.[§] The IR bands associated with adsorbed methanol increased in intensity with time, eventually reaching a steady state, as observed at 15 and 30 minutes of reaction. After 15 minutes of reaction time, when the zeolite surface is more populated with methanol, the IR bands in the 1450 to 1700 cm^{-1} region became broad and indistinguishable.

In the above experiment the effluent from the IR reaction cell was monitored for DME by MS, Fig. 10. In the first 5 minutes of the reaction negligible DME was evolved from the zeolite catalyst. This corresponds with the IR data, showing the methanol, at least in part, being scavenged to react with the benzaldehyde activated via its interaction with the BA sites. As the zeolite surface becomes more populated with methanol species DME starts to be evolved from the catalyst surface. The DME make approaches a maximum soon after the methanol coverage approaches steady-state, with the benzaldehyde promoted reaction making an order of magnitude (ca. 25-fold increase) more DME than the methanol only reaction, Fig. 10.

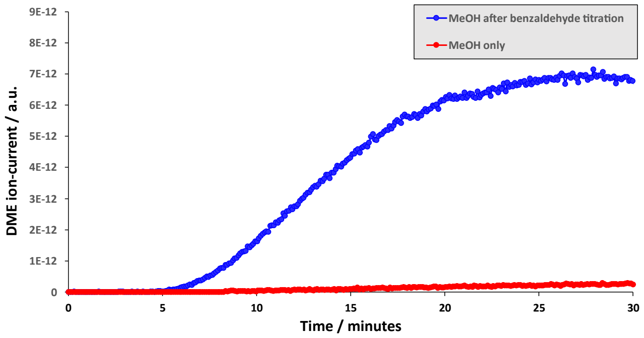

Fig. 10 DME evolved from sample of H-ZSM-5 SAR 23 at 110 °C exposed to a) methanol only, in red b) benzaldehyde, followed by methanol, in blue.

This is the case even though in both instances almost identical broad IR bands are seen in the 2800 to 3100 cm^{-1} region, due to adsorbed methanol, and any DME product that is also adsorbed on the zeolite surface. Overall, under catalytic conditions, the experiment above suggests the presence of a transient and very reactive intermediate, which undergoes a facile reaction with methanol present in the zeolite pores to give DME.

As noted previously H-ZSM-5 is reported to be an effective catalyst for the synthesis of BDA from benzaldehyde and methanol. The mechanism for the formation of acetals is widely accepted to involve the acid catalysed reaction of an alcohol (R'OH) with an aldehyde, [RC(H)(=O)], to give a hemi-acetal intermediate, [RC(H)(OH)(OR')].[34] The hemi-acetal is then protonated at the -OH group and loses water to form a transient and very reactive alkyl oxonium species, [RC(H)(C=O-R')]$^+$; this species then reacts with another molecule of alcohol to give the acetal and regenerate the proton. With this is mind DFT molecular modelling was used to simulate the IR spectrum of the methyl oxonium species which would be expected from the reaction between benzaldehyde and methanol, [PhC(H)(=O-Me)]$^+$, see ESI and Table S10. In the simulated spectra a relatively intense IR band was found at 1565 cm^{-1}, associated with IR vibrations in the C=O-Me group strongly coupled with the aromatic ring. This band is in the same locality as the distinctive band highlighted in Fig. 8.

To further support the provenance of the IR band at 1564 cm^{-1} two alternative routes were explored to generate the postulated methyl oxonium species, using H-ZSM-5 SAR 80, see Fig. 11.

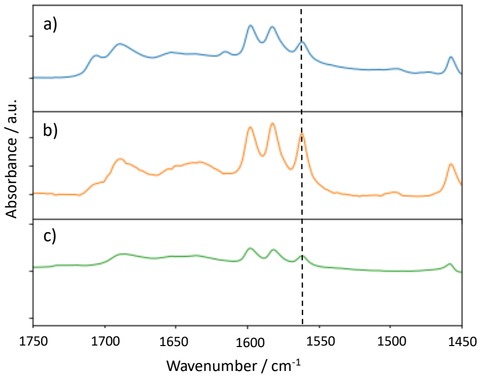

Fig. 11 FT-IR difference spectra for H-ZSM-5 SAR 80 reacted at 110 °C with a) benzaldehyde, followed by methanol b) benzaldehyde dimethyl acetal c) methanol to generate [Si(OMe)Al], followed by benzaldehyde. Black hashed line shows position of distinctive peak at 1564 cm^{-1}.

Firstly a dried sample of H-ZSM-5 SAR 80 was treated at 110 °C with a stream of N_2 saturated with BDA. This generated a similar IR spectrum to that seen when H-ZSM-5 SAR 80 was titrated with benzaldehyde and then exposed to methanol. The distinctive band at 1564 cm^{-1} was again observed, suggesting the formation of $[PhC(H)(=O\text{-}Me)]^+$ via the loss of methanol from the acetal via reaction with the zeolite BA sites. A strong IR band was also seen at 1577 cm^{-1}, previously ascribed to benzaldehyde interacting with BA sites. DME was also detected by MS in the effluent from the reaction cell. This is suggestive of a subsequent reaction between the methyl oxonium species and the liberated methanol to make DME and benzaldehyde.

In the solution phase the formation of acetals is known to be facile and readily reversible via acid catalysed hydrolysis.[34, 35] The findings here are consistent with that. Secondly a surface methoxy species, [Si(OMe)Al], was generated by firstly exposing a H-ZSM-5 SAR 80 sample to a N_2 stream saturated with methanol vapour at 110 °C, followed by removing the excess methanol and water via a N_2 purge of the reaction cell, also at 110 °C. This generated a species with distinctive IR bands at 2857 and 2957 cm^{-1}, characteristic of a surface methoxy species (SMS).[32] The SMS was then reacted with benzaldehyde by passing a N_2 stream saturated with benzaldehyde vapour over the sample at 110 °C. This again generated the distinctive band at 1564 cm^{-1}, indicating transfer of the methyl group from the SMS to the benzaldehyde C=O group to generate $[PhC(H)(=O\text{-}Me)]^+$.

The above experiments indicate that benzaldehyde promotes the M2D reaction by creating an alternative reaction pathway for the formation of DME. This pathway involves the competitive (versus methanol) adsorption of the aldehyde on a BA site, followed by reaction with methanol and loss of water to give a transient and highly reactive methyl oxonium species, which then reacts with methanol in a fast step to give DME, Scheme 1.

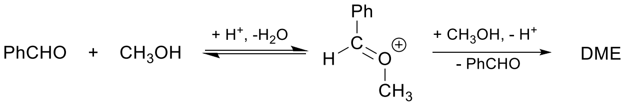

Scheme 1 Reaction pathway for benzaldehyde promoted DME formation

The formation and reactivity of the methyl oxonium species in the M2D reaction was further explored with the H-ZSM-5 SAR 80 catalyst, using the more potent 4-methylbenzaldehyde promoter tested at 110 °C. As previously the BA sites in the zeolite were first titrated with 4-methylbenzaldehyde. The sample was then exposed to methanol vapour, generating a distinctive IR band at 1554 cm^{-1}, attributed to the methyl oxonium species, $[4\text{-}Me\text{-}C_6H_4\text{-}C(H)(=O\text{-}Me)]^+$. Subsequent treatment of the sample with a stream of N_2 saturated with water vapour resulted in disappearance of the band at 1554 cm^{-1}. Re-exposure of the sample to methanol vapour regenerated the IR band at 1554 cm^{-1}. See Fig. S24 in the ESI for the IR spectra associated with these observations. This experiment demonstrates the reversible and facile nature of formation of methyl oxonium species, as shown in Scheme 1, but in this case for 4-methylbenzaldehyde.

The facile nature of the reactions described above indicates that under catalysis conditions the methyl oxonium species is in a rapid pre-equilibrium with the reactants and is present at very low concentrations when excess methanol is present. The proposed pathway is also consistent with the inhibitory effect of added water on promoter effectiveness, as observed in the catalytic tests. As noted previously the above pathway is related to the one proposed for the acid catalysed formation and hydrolysis of acetals in solution. The formation and hydrolysis of aromatic acetals is promoted by electron-donating groups, which stabilize the highly reactive alkyl oxonium intermediate, $[ArC(H)(C=O\text{-}R)]^+$.[34] This, at least in part, explains the reactivity trend seen in Fig. 4.

There is, however, an additional factor in play in determining promoter potency, related to the solvating effect of the zeolite pore walls on reaction intermediates and transition states. To explore this aspect further the potent 4-n-pentylbenzaldehyde promoter was tested as a promoter for the M2D reaction with H-ZSM-5 SAR 23 in the FT-IR-MS high temperature reaction cell, Fig. 12. As previously the zeolite BA sites were first titrated with the aldehyde, see ESI and Fig. S27. Strong IR bands at 1596 and 1578 cm^{-1} were observed, assigned to strongly coupled C=O and aromatic ring vibrations in the protonated aldehyde. IR bands at 1629 and 1675 cm^{-1} were also present, due to the vibrations from the aldehyde C=O group interacting with LA sites and silanol -OH groups. The M2D reaction was then initiated by passing methanol vapour over the zeolite catalyst. The M2D reaction was continued for 2 hours and the FT-IR spectrum at this point indicated the presence of a methyl oxonium species, $[4\text{-}n\text{-}pentyl\text{-}C_6H_4C(H)(=O\text{-}Me)]^+$ with a distinctive IR at band 1547 cm^{-1}, despite the zeolite surface being populated with methanol species (IR bands in the 2800 to 3100 cm^{-1} region). The sample was then purged with N_2 to remove excess methanol and any water and DME product adsorbed on the zeolite surface. After the N_2 purge the distinctive IR band at 1547 cm^{-1}, due to the methyl oxonium species, was still present. The IR bands due to the aldehyde weakly interacting with the LA sites and silanol -OH groups were however absent, indicating that during the M2D reaction the methanol had displaced the aldehyde from these sites. The prominence and longevity of the promoter IR bands associated with the BA sites during this M2D experiment illustrates the anchoring effect of the pendant n-pentyl group on promoter competitive adsorption versus methanol, via zeolite pore wall induced van der Waal forces cf. Fig. 9 with benzaldehyde.

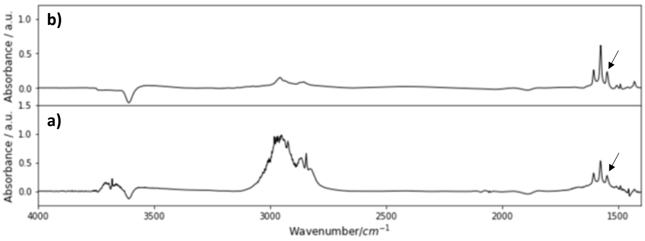

Fig. 12 FT-IR difference spectra for H-ZSM-5 SAR 23 at 110 °C after a) titration with 4-n-pentylbenzaldehyde, followed by reaction with methanol, spectrum shown after 2 hours of reaction b) purging with N_2 after the M2D reaction. Black arrow shows position of distinctive peak at 1547 cm^{-1}.

Molecular modelling studies

Reaction mechanism and key steps Molecular modelling was used to further explore the reaction pathway and mechanism discussed above for the benzaldehyde promoted M2D reaction with H-ZSM-5. A simplified reaction mechanism showing the key DME forming step is shown in Scheme 2; see Scheme S1 in the ESI for the full reaction pathway and mechanism.

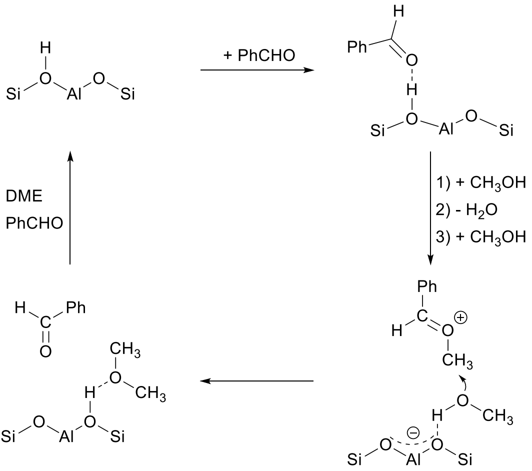

Scheme 2 Simplified reaction mechanism for benzaldehyde promoted zeolite catalysed methanol dehydration to DME. The interaction of the reactants with the zeolite BA site, [Si(OH)Al], is shown.

For the molecular modelling simulations a representative BA site was selected at the intersection of the straight and sinusoidal channels of ZSM-5 (MFI), selecting the O2 site located between the T1 and T2 sites with the T1 site selected for the Al location. The adsorption of benzaldehyde on this BA site was then modelled using two modes of adsorption, Fig. 13. The first adsorption mode involved a H-bonding interaction of the benzaldehyde carbonyl group with the BA site, with the formyl group (CHO) twisted out of the plain with the phenyl ring. Multiple initial conformations were tested, with the one reported here being the lowest energy conformer found. In the H-bonded adsorption mode the electron-rich aromatic ring is aligned with the ellipsoidal straight pore of ZSM-5, with the aromatic ring located at the centre of the pore. After geometry optimization this gave an adsorption energy of -143 kJ mol^{-1}, despite the energy penalty being paid by breaking conjugation between the formyl group and the phenyl ring. Once optimized the O-C-C-C dihedral angle had a value of 83.6 degrees and the C=O group H-bond distance was 1.39 Å, indicating a strong hydrogen bonding interaction. In the second adsorption mode the proton was desorbed from the BA site and placed on the oxygen of the formyl group, with the positively charged molecule kept planar and similarly placed in the centre of the zeolite pore. In this case the protonated formyl group retained its conjugation with the aromatic ring. This gave an adsorption energy of -130 kJ mol^{-1}, which despite being conjugated, was 13 kJ mol^{-1} less than found for the H-bonded mode of adsorption. The energy difference between the two modes of adsorption is however relatively small. The experimentally measured energy barrier for the rotation of the formyl group in benzaldehyde in the vapour and liquid phases is reported to be between 19 and 33 kJ mol^{-1}.[36]

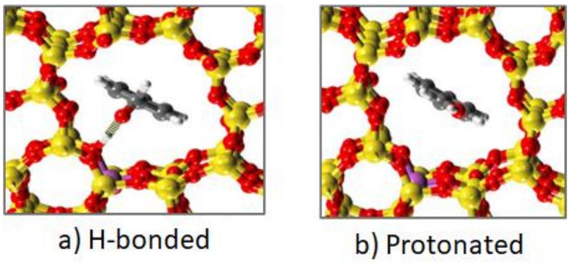

Fig. 13 Benzaldehyde adsorption modes on H-ZSM-5 via a) H-bonding to the BA site b) deprotonation of the BA site.

Benzaldehyde adsorbed in the H-bonded mode was selected as the starting point for completing the rest of the catalytic cycle and calculation of the energies of intermediates and transition states. Reasonable transition states were identified for the formation of the hemi-acetal intermediate and its dehydration to give the methyl oxonium species, Fig. 14.

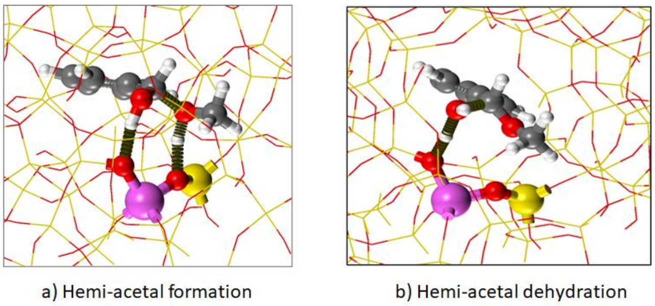

Fig. 14 Transition states identified for a) the formation of the hemi-acetal intermediate via reaction between adsorbed benzaldehyde and methanol and b) subsequent dehydration of the hemi-acetal intermediate to give the methyl oxonium species plus adsorbed water, via a H-bonding interaction with the BA site. Pink atom Al, yellow atom Si, red atoms O, grey atoms carbon and white atoms H.

A transition state for the key DME forming step, involving a S_N2 reaction of the methyl oxonium species with an adsorbed methanol, as shown in Scheme 2, was also identified, Fig. 15.

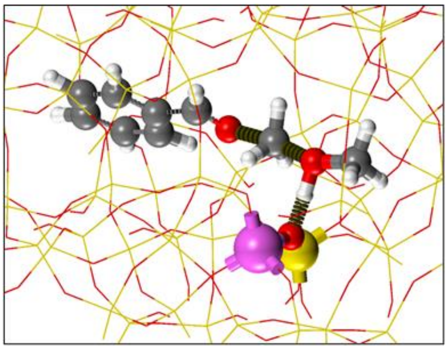

Fig. 15 Transition state identified for the reaction of a benzaldehyde derived methyl oxonium species with absorbed methanol, resulting in the formation of DME H-bonded to a BA site. Pink atom Al, yellow atom Si, red atoms O, grey atoms C and white atoms H.

The full reaction coordinate diagram with associated energies is given in Fig. S37 in the ESI. The apparent activation energy barrier for the overall catalytic cycle is 88 kJ mol^{-1} and is associated with the reaction of the methyl oxonium species with adsorbed methanol to give DME adsorbed on a BA site, transition state 3 in Fig. S37. The molecular modelling findings here illustrate a reasonably plausible pathway and mechanism for the role of benzaldehyde in promoting the M2D reaction with H-ZSM-5 and by extension with other zeolites.

The reaction energetics shown in Fig. S37 are solely based upon electronic energy contributions at zero kelvin. Entropy contributions, which are no doubt significant for chemistry occurring in the confines of a zeolite pore, were not considered as currently available methods do not allow for calculating entropy contributions accurately with such complex systems (in a microporous network with several adsorbed molecules).[33, 37] In addition the findings presented here do not exclude other reaction pathways, for example involving the reaction of protonated benzaldehyde species to form the hemi-acetal intermediate, which may occur instead or in parallel, and may more favourably occur when electron-donating substituents are present on the aromatic ring. The reaction steps modelled here also involve static simulations and are performed in the absence of excess methanol, DME and water. Under the high coverage and dynamic conditions of actual catalysis, where protonated methanol clusters and other solvated species can be present, the situation is undoubtedly more complex. Molecular dynamic simulations using protonated methanol clusters,[38] interacting with the aldehyde promoter, BA sites and other species may prove to be informative here but that is beyond the scope of the initial findings presented in this paper.

Gas phase protonation and methylation energies Molecular modelling was used to determine the gas phase protonation and methylation energies (see Table S9 in the ESI) of benzaldehyde and the 3- and 4-substituted benzaldehyde derivatives tested as promoters for the M2D reaction. $[H_3O]^+$ and $[MeOH_2]^+$ were used as the protonating and methylating reagents, Scheme 3.

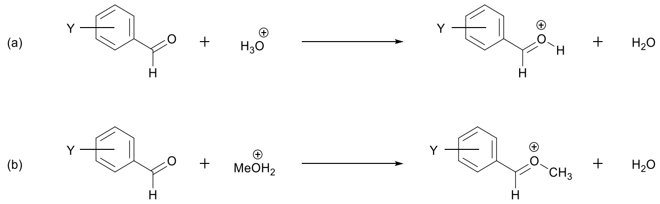

Scheme 3 Gas phase reactions of benzaldehyde and its derivatives via a) protonation with $[H_3O]^+$ and b) methylation with $[MeOH_2]^+$.

The Hammett constant, σ, based on the dissociation constant of benzoic acid and its 3- and 4-substiuted derivatives, is widely used in organic chemistry to predict and evaluate reactivity trends.[1] The calculated gas phase aldehyde protonation and methylation energies were hence compared with the Hammett constant, Fig. 16. There is reasonably good correlation between the methylation and protonation energies and the Hammett constant. Electron-donating groups (negative σ values) were found to favour the methylation and protonation reactions, whilst both reactions were generally, though not in all cases, disfavoured by electron-withdrawing groups (positive σ values).

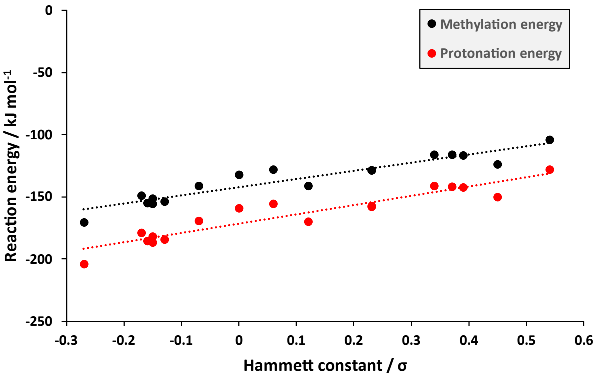

Fig. 16 Reaction energies versus the Hammett constant, σ_m or σ_p, for the gas phase protonation and methylation reactions of benzaldehyde and 3- and 4-substituted benzaldehyde derivatives using a) $[H_3O]^+$ as a protonating agent and b) $[MeOH_2]^+$ as a methylating agent. σ = 0 for benzaldehyde.

Promoter zeolite adsorption energies We have previously shown that the adsorption energy of aliphatic methyl esters, RCO_2Me, on a zeolite BA site can act as a reasonable guide for promoter potency.[10] With this in mind molecular modelling was used to determine the adsorption energy of benzaldehyde relative to some of the 4-substituted benzaldehyde derivatives tested for the M2D reaction. The same methodology as described above for benzaldehyde was employed, with the benzaldehyde derivative either H-bonded to the BA site or fully protonated by the BA site. The calculated adsorption energies are shown in Fig. 17.

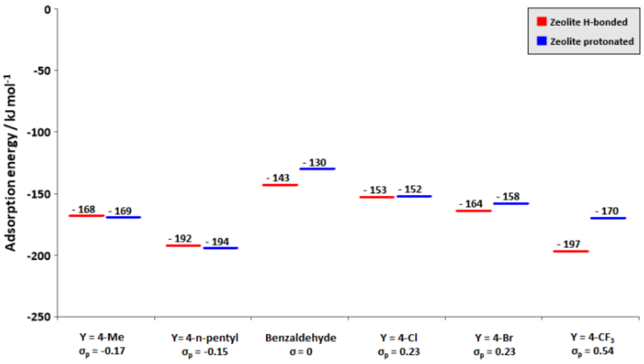

Fig. 17 Relative adsorption energies for benzaldehyde and 4-substituted benzaldehyde derivatives, 4-Y-C_6H_4CHO, absorbed on a BA site in H-ZSM-5 via a) H-bonding, lines in red or b) protonation, lines in blue. Experimental Hammett constants σ_p shown relative to benzaldehyde, $\sigma = 0$.

The calculated zeolite adsorption energies do not follow a trend that might be expected from the Hammett constant and the general trend observed above for the gas phase aldehyde protonation reaction. In the series shown the benzaldehyde derivative with the most strongly electron-withdrawing substituent, 4-CF_3 with a σ_p of 0.54, is found to adsorb the strongest when bound in the H-bonded unconjugated form. Somewhat surprisingly 4-CF_3-benzaldehyde also absorbs relatively strongly in the conjugated protonated form. 4-n-pentylbenzaldehyde also adsorbs very strongly; the H-bonded form was found to have an adsorption energy of -192 kJ mol^{-1}, whilst the protonated form was found to have an adsorption energy of -194 kJ mol^{-1}. These adsorption energies are significantly above those calculated for 4-methylbenzaldehyde, of -168 kJ mol^{-1} for the H-bonded form, and -169 kJ mol^{-1} for the protonated form. In addition of all the aldehydes evaluated in Fig. 17 benzaldehyde adsorbs the weakest, irrespective of whether it is adsorbed in either the protonated or the H-bonded form. These findings indicate that the solvating effect of the zeolite pore walls on the substituents on the aromatic ring has a significant impact on adsorption energy of the aldehyde promoters, over what might be expected purely from the electron-withdrawing and -donating effects of the substituents on the aromatic ring. The relative adsorption energies do however reflect the observation that the substituted benzaldehyde M2D promoters all approach saturation kinetics at lower concentrations than benzaldehyde, *vide supra*. All the aldehydes evaluated adsorbed more strongly than methanol, which had an adsorption energy of -118 kJ mol^{-1} when H-bonded to the same BA site.

In Fig. 17 the largest difference between the zeolite H-bonded and protonated benzaldehyde derivatives is seen for 4-CF_3-benzaldehyde, with an energy gap of 27 kJ mol^{-1} in favour of the H-bonded form. The strongly electron-withdrawing 4-CF_3 group disfavours the protonated mode of adsorption for this aldehyde, in line with expectations. For 4-Me-benzaldehyde the energy gap between the H-bonded and protonated forms was negligible, at 1 kJ mol^{-1}, being slightly in favour of the protonated form. Similarly, 4-Cl-benzaldehyde, which also adsorbed more strongly than benzaldehyde, had a negligible energy gap of 1 kJ mol^{-1}, between the zeolite protonated and H-bonded forms, this time slightly in favour of the H-bonded form. As noted previously for benzaldehyde the H-bonded form was favoured by 13 kJ mol^{-1} over the protonated form of the adsorbed aldehyde.

In terms of the adsorption energies shown for 4-n-pentylbenzaldehyde in Fig. 17 it should be noted that the conformation that the n-pentyl group adopts with respect to the aromatic ring, along with the overall aldehyde orientation and location in the zeolite pore, does have an impact on the adsorption energy calculated; see the ESI and Fig. S36 for two examples. In Fig. 17 the adsorption energy shown is therefore illustrative of the general trend expected on increasing the length of the alkyl group in the 4-position of benzaldehyde. The finding here is however in alignment with the higher potency of the 4-n-pentylbenzaldehyde M2D promoter, as demonstrated for the catalytic data shown in Fig. 5. The absorption energies reported in this paper use a representative BA site at the intersection of the straight and sinusoidal channels of ZSM-5. These static simulations are instructional rather than absolute, as many other possibilities exist for promoter adsorption in the zeolite pores e.g. choice of BA site location, aldehyde in protonated or H-bonded form, and the overall promoter conformation and orientation with respect to the zeolite pore walls. The calculations do however illustrate that zeolite solvation effects play a critical role in the adsorption strength of promoters and by extension the energies of reaction intermediates and transition states.

Promoter descriptor generation and correlation analysis

Given the complexities discussed above, to further explore the influence of aromatic aldehyde promoter structure on the H-ZSM-5 catalysed M2D reaction it was decided to employ the data analytics approach developed by Sigman and co-workers[39-44] and used by others.[45-47] The rotational conformers for benzaldehyde and its derivatives were subjected to geometry optimisation by DFT at the B3LYP/def2-TZVP level of theory. The lowest energy conformer was selected, and steric and electronic descriptors for the promoters were extracted to build a dataset for further analysis. The extracted parameters were the molecular dipole moment (μ), isotropic and anisotropic polarizability (^{iso}Pol and $^{aniso}Pol$), infrared carbonyl stretching frequency ($V_{C=O}$), HOMO and LUMO energies, and natural bond orbital (NBO)[48-51] charges of each atom (C, H and O) in the aldehyde group. Molecular volume (*MV*) and molecular surface area (*S*) data together with relative molecular mass (M_r) and Hammett values (σ_p *or* σ_m)[1] were also collected (see Table S5 in the ESI). The Verloop Sterimol parameters B_1, B_5, and L,[52, 53] for ring substituents, were calculated for the geometry optimized structures, using the MORFEUS package (Table S6 in the ESI).[54]

The correlation between the molecular descriptors determined for benzaldehyde and its 3- and 4-substituted derivatives and DME STY for the promoted M2D reaction was then explored, using the DME STY data collected at 150 °C for H-ZSM-5 SAR 80. The Pearson correlation coefficient was calculated using KNIME,[55] and a univariate correlation matrix heatmap generated, see Fig. 18 and ESI Table S12.

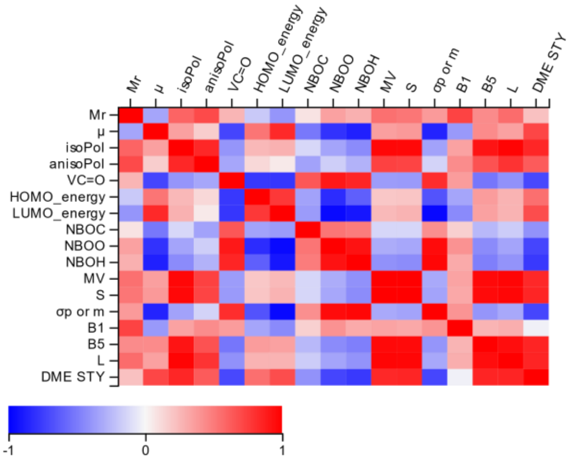

Fig. 18 Pearson correlation heatmap for aldehyde molecular descriptors and DME STY (g kg^{-1}h^{-1}) for H-ZSM-5 SAR 80 catalysed methanol dehydration at 150 °C, promoted by 0.01 mol % of benzaldehyde and 3- and 4-substituted benzaldehyde.

As expected, many of the electronic parameters are highly correlated, as shown graphically in Fig. 18. There is a moderate linear correlation ($R^2 = 0.67$) between $V_{C=O}$ and the Hammett constant values of benzaldehyde and its 3- and 4-substituted derivatives, see Fig. S42 in the ESI. In Fig. S42 there is however a much stronger linear relationship between the Hammett constant and both the LUMO energy ($R^2 = 0.94$) and the NBO charge on the carbonyl group oxygen ($R^2 = 0.91$). These findings indicate that DFT derived electronic parameters can be used in place of Hammett values, as has been previously reported.[56-58] Additionally, ^{iso}Pol, molecular surface area (S), B_5 and L are highly correlated (R^2 values above 0.92; see ESI Fig. S43 for an example). The best univariate correlations with DME STY were obtained with Sterimol parameters L and B_5 ($R^2 = 0.73$) together with ^{iso}Pol and molecular surface area (S) ($R^2 = 0.72$), see ESI Fig. S45. This is consistent with the substituent size having a strong influence on the solvating effect of the zeolite pores on the energy of intermediates and transition states. Correlation of DME STY with electronic descriptors NBO_O, LUMO energy, $V_{C=O}$, μ, and σ_p *or* $_m$ is lower, with R^2 values below 0.6, see Fig. S46 and Fig. S47 in the ESI . With this data in hand it was decided to use multivariate linear regression analysis to construct an interpretable model for DME STY with H-ZSM-5 SAR 80 at 150 °C, when tested with 0.01 mol % of benzaldehyde and its mono-substituted derivatives.

Multivariate linear regression (MLR) analysis

The forward stepwise regression feature in JMP,[59] was used to build models for DME STY, using DME STY data from Table S2 and normalised descriptors for benzaldehyde and 3- and 4-substituted benzaldehyde derivatives. The models were analysed using standard metrics (RMSE and R2). Due to the small size of the dataset cross-validation was performed using the leave-one-out (LOO) method.[60] The LUMO energy and L were selected as the most important variables to build the DME STY model upon. An excellent correlation (R2 = 0.95) was observed with just these two parameters, that describe the steric and electronic properties of the benzaldehyde promoter molecules, Fig. 19. Predicted values and full model details are presented in the ESI. In the DME STY model shown in Fig. 19 the substituent length (Sterimol parameter L) acts as an approximation for the solvating effect of the zeolite pores on the energy of intermediates and transition states. The LUMO energy contribution in the model reflects the electronic influence of the ring substituents in stabilizing protonated and methylated oxonium species. Cross-validation (LOO = 0.94) indicates a robust model. Due to the high level of correlation between electronic and steric features similar DME STY models, for the M2D reaction with benzaldehyde and its 3- and 4-substituted derivatives, can also be obtained using either NBOO or Hammett values combined with L or molecular surface area, see Section S7.7 in the ESI.

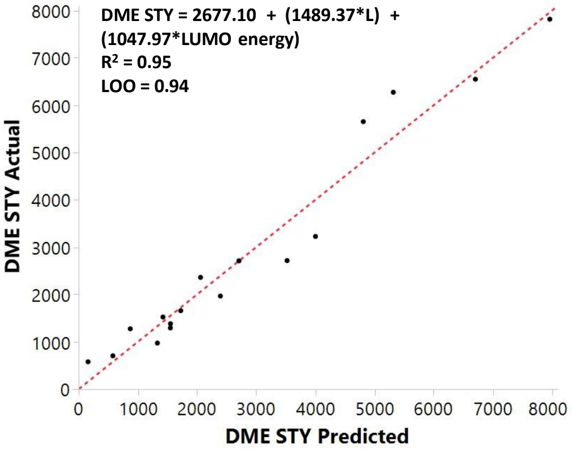

Fig. 19 Multivariate model for DME STY (g $kg^{-1}h^{-1}$), actual versus predicted values, for the H-ZSM-5 SAR 80 catalysed M2D reaction at 150 °C, promoted by 0.01 mol % of benzaldehyde and 3- and 4-substituted benzaldehyde derivatives.

The model above for ZSM-5 SAR 80 was extended to include the 2-substituted benzaldehyde derivatives tested in Table S3. A high correlation for DME STY was obtained with a model using just L and the LUMO energy as variables (R^2 = 0.90, see ESI Fig. S53). However prediction accuracy for benzaldehyde, 2-methyl-benzaldehyde and 2-methoxybenzaldehyde was low. The model and prediction, Fig. 20, was improved by adding the B_{5ortho} Sterimol parameter,[56] which describes the maximum width of the substituent in the 2-position. The same form of model could be applied to aromatic aldehyde promotion of the M2D reaction with another 3-dimensional zeolite, H-ZSM-11 SAR 50, when tested at 150 °C, Fig. 20.

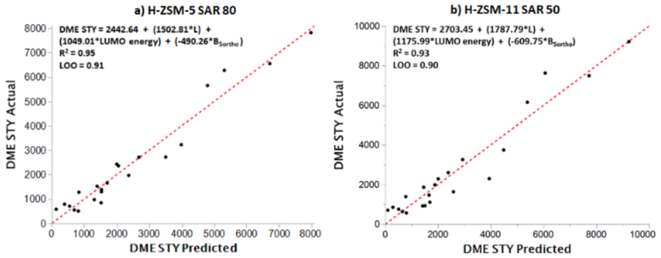

Fig. 20 Multivariate regression model for DME STY (g $kg^{-1}h^{-1}$), actual versus predicated values, for the a) H-ZSM-5 SAR 80 and b) H-ZSM-11 SAR 50 catalysed M2D reaction at 150 °C, using 0.01 mol % of benzaldehyde and 2-, 3- and 4-substituted benzaldehyde derivatives as promoters.

It should be noted that alternative models can be built with the available data, yielding similar DME STY predictions by combining different molecular descriptors; see the ESI for some examples. Incorporating non-linear effects could also potentially result in better model predictions. However, we favour a simple linear model using 2 or 3 interpretable molecular descriptors as variables. The models generated here reflect the importance of the size and shape of the aldehyde promoter as well as the electronic effects of the aromatic ring substituent in determining promoter potency.

Conclusions

Benzaldehyde and its derivatives have been found to be effective promoters for zeolite catalysed methanol dehydration to DME at low temperature (110 to 150 ^oC). For the 3-dimensional medium pore zeolite H-ZSM-5 (MFI) the promotion is readily reversible, and the potency of the promoter can be tuned by varying the substituent on the aromatic ring of the aldehyde. The most potent promoters are active at concentrations as low as 0.0001 mol % (1 ppm) relative to methanol. In this study high throughput experimentation (HTE) is used to screen and rank potential promoters and catalysts and to collect high quality kinetic data for the most promising candidates discovered. The catalytic data and *in-situ* FT-IR-MS experiments combined with molecular modelling studies indicate a mechanism involving competitive adsorption of the aldehyde promoter on a Brønsted acid site, followed by reaction with methanol to give a hemi-acetal intermediate. Loss of water from the hemi-acetal intermediate generates a transient and highly reactive methyl oxonium species, $[ArC(H)(=O\text{-}Me)]^+$, which then directly reacts with methanol via a S_N2 mechanism to give DME and regenerate the aldehyde promoter and BA site. The methyl oxonium species is stabilized by electron-donating groups on the aromatic ring and the solvent like effect of the zeolite pore walls. Molecular descriptors were calculated by molecular modelling for the 22 aromatic aldehyde promoters tested. Multivariate linear regression analysis was used to build an interpretable model for aldehyde promotional activity in H-ZSM-5 and in another 3-dimensional medium pore zeolite, H-ZSM-11 (MEL). It is often said that the solvent like effect of micropores in zeolite catalysts imparts enzyme like properties. The most effective promoters described here have biological-like potency, being active at concentrations as low as 1 ppm. The kinetic behaviour seen in the FT-IR-MS experiments, involving a short induction period to establish a rapid pre-equilibrium between reactants and the Brønsted acid active site, forming a steady-state but low concentration of a highly reactive methyl oxonium intermediate, is very reminiscent of Michaelis-Menten enzyme kinetics.[61]

Zeolites are increasingly being used for the processing of biomass derived feedstocks, often in the presence of significant amounts of water.[25, 26, 62] Davis and co-workers have recently shown that grafting phenethyl-sulfonic acid sites into the micropores of the wide pore zeolite H-beta gives a very efficient catalyst for the hydroxyalkylation/alkylation condensation reaction of 2-methylfuran with acetone.[23] This increased catalytic efficiency results from the confinement effect of the zeolite micropores, combined with increased hydrophobicity imparted by the grafting sulfonic acid containing residues into silica-rich micropores. The grafted sulfonic acid contains an aromatic ring and a linking alkyl chain, with a reactive sulfonic acid head-group placed on the aromatic ring. Here we show that benzaldehyde derivatives, containing an alkyl chain in the 4-position and a reactive formyl head-group, can have a similar effect on the zeolite catalysed M2D reaction when just simply added to the methanol feed. Given that biomass derived molecules are rich in oxygen containing functional groups, it is possible that similar chemistry may also occur when these molecules are co-processed with alcohols[31, 62, 63] using zeolite catalysts, impacting the reaction pathway and overall process yield of the alcohols used.

This paper shows that the confinement effect in zeolite catalysts can magnify the effect of extremely low levels of organic compounds, including impurities, when they are present in chemical feedstocks and process recycle streams. In the work described here, where the M2D aromatic aldehyde promoters are deliberately added to the methanol feed, this can have a positive impact on zeolite catalyst performance. In other circumstances however, organic impurities, especially strongly adsorbing ones present even at ppm level concentrations, may result in undesirable process chemistry e.g. via a detrimental impact on selectivity and/or catalyst lifetime. Industrially this has significance in the cleaning-up of biomass derived feedstocks to ensure commercially attractive catalyst performance is maintained over the lifetime of a zeolite catalyst. In fundamental work, aimed at understanding structure-property relationships, it shows the importance of understanding the impact reagent purity has on reproducibility, via reagent analysis, and the use of frequently repeated control experiments. It is also important that HTE testing equipment is effectively cleaned and purged to remove contaminants from previous experiments, to ensure that high quality and reliable data is collected for model building.

Lastly fundamental studies on the role of aromatic compounds in methanol to hydrocarbons (MTH) chemistry have historically focussed on the role of methylated benzenes in the hydrocarbon pool mechanism. The results presented here highlight the possibility that under certain circumstances oxygen containing aromatic residues in zeolite pores may also play an underlying role in MTH and other chemistries by moderating the reaction pathway.

Author Contributions

Conceptualisation G.J.S.; promoter and catalyst discovery G.J.S., Z.Y., B.D.S.; experimental design for reaction kinetics and promoter ranking, Z.Y., F.J., B.D.S, G.J.S; high-throughput catalyst and promoter testing, A.E., N.S., X. T.; FT-IR studies, Z.X., Z.Y, with input from G.J.S; molecular modelling, C.B., G.A.P.; reaction mechanism, G.J.S, C.B.; multivariate linear regression, G.A.P.; G.J.S. wrote the manuscript with the support of Z.X., C.B., G.A.P.

Conflicts of interest

The work reported here is the subject of a patent application.[22]

Affiliations & corresponding author

[a] *Applied Sciences, bp Innovation & Engineering, Energy Innovation Laboratory, BP Office (Dalian Institute of Chemical Physics), BP plc, Dalian, China.*
[b] *Applied Sciences, bp Innovation & Engineering, BP plc, Saltend, Hull, HU12 8DS, United Kingdom. * E-mail: glenn.sunley@uk.bp.com*
[c] *Applied Sciences, bp Innovation and Engineering, BP plc, 30 South Wacker Drive, Chicago, IL 60606, United States of America.*

Acknowledgements

We thank BP plc for funding and permission to publish this work. We thank Dr. Nikos Diamantonis, Dr. Mark Sankey and Dr. Tom Lakey for dew point calculations. Christopher Owens, Ning Wang and John Bramlet are thanked for assistance with additional experiments. We thank Dr. Pan Gao and Prof. Guangjin Hou at Dalian Institute of Chemical Physics, Chinese Academy of Sciences, for technical assistance in conducting preliminary NMR experiments. Dr. Xuebin Liu and Prof. Christophe Copéret are thanked for helpful discussions.

Notes and references

‡ See ESI for how IR band assignments were determined.

§ Preliminary *in-situ* solid state NMR experiments with H-ZSM-5, benzaldehyde and ^{13}C-enriched methanol indicate that very low levels of DME are formed on the surface of the zeolite at ambient temperature, with more significant amounts formed at 65, 95 and 110 ^{o}C. See ESI for details.

1. C. Hansch, A. Leo and R. W. Taft, *Chem. Rev.*, 1991, **91**, 165-195.
2. M. Stradiotto and R. J. Lundgren, *Ligand Design in Metal Chemistry: Reactivity and Catalysis*, 2016.
3. G. J. P. Britovsek, V. C. Gibson and D. F. Wass, *Angewandte Chemie - International Edition*, 1999, **38**, 429-447.
4. G. J. P. Britovsek, S. P. D. Baugh, O. Hoarau, V. C. Gibson, D. F. Wass, A. J. P. White and D. J. Williams, *Inorg. Chim. Acta*, 2003, **345**, 279-291.
5. D. F. Wass, *Journal of the Chemical Society. Dalton Transactions*, 2007, 816-819.
6. O. M. Ogba, N. C. Warner, D. J. O'Leary and R. H. Grubbs, *Chem. Soc. Rev.*, 2018, **47**, 4510-4544.
7. C. A. Carraz, E. J. Ditzel, A. G. Orpen, D. D. Ellis, P. G. Pringle and G. J. Sunley, *Chem. Commun.*, 2000, 1277-1278.
8. E. G. Derouane, *J. Mol. Catal. A: Chem.*, 1998, **134**, 29-45.
9. S. Abate, K. Barbera, G. Centi, P. Lanzafame and S. Perathoner, *Catalysis Science & Technology*, 2016, **6**, 2485-2501.
10. B. J. Dennis-Smither, Z. Yang, C. Buda, X. Liu, N. Sainty, X. Tan and G. J. Sunley, *Chem. Commun.*, 2019, **55**, 13804-13807.
11. B. E. Langner, *Appl. Catal.*, 1982, **2**, 289.
12. T. Mole, G. Bett and D. Seddon, *J. Catal.*, 1983, **84**, 435.
13. S. Kolboe, *Stud. Surf. Sci. Catal.*, 1988, **36**, 189.
14. I. M. Dahl and S. Kolboe, *Catal. Lett.*, 1993, **20**, 329.
15. M. Stocker, *Microporous Mesoporous Mater.*, 1999, **29**, 3-48.

16. J. F. Haw, W. Song, D. M. Marcus and J. B. Nicholas, *Acc. Chem. Res.*, 2003, **36**, 317-326.
17. U. Olsbye, S. Svelle, K. P. Lillerud, Z. H. Wei, Y. Y. Chen, J. F. Li, J. G. Wang and W. B. Fan, *Chem. Soc. Rev.*, 2015, **44**, 7155-7176.
18. A. D. Chowdhury, A. L. Paioni, K. Houben, G. T. Whiting, M. Baldus and B. M. Weckhuysen, *Angew. Chem. Int. Ed.*, 2018, **57**, 8095-8099.
19. I. Lezcano-Gonzalez, E. Campbell, A. E. J. Hoffman, M. Bocus, I. V. Sazanovich, M. Towrie, M. Agote-Aran, E. K. Gibson, A. Greenaway, K. De Wispelaere, V. Van Speybroeck and A. M. Beale, *Nature Materials*, 2020, **19**, 1081-1087.
20. Z. Azizi, M. Rezaeimanesh, T. Tohidian and M. R. Rahimpour, *Chemical Engineering and Processing: Process Intensification*, 2014, **82**, 150-172.
21. Q. Zhang, J. Yu and A. Corma, *Adv. Mater.*, 2020, **32**, 2002927.
22. B. J. Dennis-Smither, J. G. Sunley and Z. Yang, WO2020168539, 2020, to BP P.L.C. and BP China Holdings Ltd.
23. M. Lusardi and M. E. Davis, *ACS Sustainable Chemistry & Engineering*, 2021, **9**, 17120-17127.
24. M. V. Joshi and C. S. Narasimhan, *J. Catal.*, 1991, **128**, 63-68.
25. R. Gounder and M. E. Davis, *AlChE J.*, 2013, **59**, 3349-3358.
26. R. Gounder, *Catal. Sci. Technol.*, 2014, **4**, 2877-2886.
27. I. Ahmad, J. A. Anderson, T. J. Dines and C. H. Rochester, *J. Colloid Interface Sci.*, 1998, **207**, 371-378.
28. I. Ahmad, J. A. Anderson, C. H. Rochester and T. J. Dines, *J. Mol. Catal. A: Chem.*, 1998, **135**, 63-73.
29. G. B. Tolstorozhev, I. V. Skornyakov, M. V. Bel'kov, O. I. Shadyro, S. D. Brinkevich and S. N. Samovich, *Opt. Spectrosc.*, 2012, **113**, 179-183.
30. P. Hoffmann and J. A. Lobo, *Microporous Mesoporous Mater.*, 2007, **106**, 122-128.
31. P. Lanzafame, G. Papanikolaou, S. Perathoner, G. Centi, M. Migliori, E. Catizzone, A. Aloise and G. Giordano, *Catalysis Science & Technology*, 2018, **8**, 1304-1313.
32. T. R. Forester and R. F. Howe, *J. Am. Chem. Soc.*, 1987, **109**, 5076-5082.
33. A. J. Jones and E. Iglesia, *Angew. Chem., Int. Ed.*, 2014, **53**, 12177-12181.
34. T. S. Davis, P. D. Feil, D. G. Kubler and D. J. Wells, Jr., *The Journal of Organic Chemistry*, 1975, **40**, 1478-1482.
35. E. H. Cordes, *Prog. Phys. Org. Chem.*, 1967, **4**, 1-44.
36. G. H. Penner, P. George and C. W. Bock, *Journal of Molecular Structure: THEOCHEM*, 1987, **152**, 201-212.
37. P. Deshlahra and E. Iglesia, *Chem. Commun. (Cambridge, U. K.)*, 2020, **56**, 7371-7398.
38. S. A. F. Nastase, P. Cnudde, L. Vanduyfhuys, K. De Wispelaere, V. Van Speybroeck, C. R. A. Catlow and A. J. Logsdail, *ACS Catal.*, 2020, **10**, 8904-8915.
39. C. B. Santiago, J.-Y. Guo and M. S. Sigman, *Chemical Science*, 2018, **9**, 2398-2412.
40. M. S. Sigman, K. C. Harper, E. N. Bess and A. Milo, *Acc. Chem. Res.*, 2016, **49**, 1292-1301.
41. J. P. Reid and M. S. Sigman, *Nature Reviews Chemistry*, 2018, **2**, 290-305.
42. J. M. Crawford, T. Gensch, M. S. Sigman, J. M. Elward and J. E. Steves, *Organic Process Research & Development*, 2022, **26**, 1115-1123.
43. M. A. B. Ferreira, J. De Jesus Silva, S. Grosslight, A. Fedorov, M. S. Sigman and C. Copéret, *J. Am. Chem. Soc.*, 2019, **141**, 10788-10800.
44. P. S. Engl, C. B. Santiago, C. P. Gordon, W. C. Liao, A. Fedorov, C. Copéret, M. S. Sigman and A. Togni, *J. Am. Chem. Soc.*, 2017, **139**, 13117-13125.
45. S. H. Lau, M. A. Borden, T. J. Steiman, L. S. Wang, M. Parasram and A. G. Doyle, *J. Am. Chem. Soc.*, 2021, **143**, 15873-15881.
46. B. Maity, Z. Cao, J. Kumawat, V. Gupta and L. Cavallo, *ACS Catalysis*, 2021, **11**, 4061-4070.
47. D. J. Durand and N. Fey, *Acc. Chem. Res.*, 2021, **54**, 837-848.
48. A. E. Reed, R. B. Weinstock and F. Weinhold, *The Journal of Chemical Physics*, 1985, **83**, 735.
49. F. Weinhold, *J. Comput. Chem.*, 2012, **33**, 2363-2379.
50. E. D. Glendening, C. R. Landis and F. Weinhold, *Computational Molecular Science*, 2012, **2**, 1-42.
51. NBO, E. D. Glendening, J. K. Badenhoop, A. E. Reed, J. E. Carpenter, J. A. Bohmann, C. M. Morales and F. Weinhold, *(Theoretical Chemistry Institute, University of Wisconsin, Madison, WI)*, 2001.
52. A. Verloop, in *Pesticide Chemistry: Human Welfare and Environment*, eds. P. Doyle and T. Fujita, Pergamon, 1983, pp. 339-344.
53. A. Verloop, W. Hoogenstraaten and J. Tipker, in *Drug Design*, ed. E. J. Ariëns, (Academic Press), 1976, vol. 11, pp. 165-207.
54. K. Jorner, MORFEUS, https://github.com/kjelljorner/morfeus).
55. M. R. Berthold, N. Cebron, F. Dill, T. R. Gabriel, T. Kötter, T. Meinl, P. Ohl, C. Sieb, K. Thiel and B. Wiswedel, in *KNIME: The Konstanz Information Miner in Data Analysis, Machine Learning and Applications. Studies in Classification, Data Analysis, and Knowledge Organization.*, eds. C. Preisach, H. Burkhardt, L. Schmidt-Thieme and R. Decker, Springer Berlin Heidelberg, Berlin, Heidelberg, 2008, pp. 319-326.
56. C. B. Santiago, A. Milo and M. S. Sigman, *J. Am. Chem. Soc.*, 2016, **138**, 13424-13430.
57. C. A. Hollingsworth, P. G. Seybold and C. M. Hadad, *Int. J. Quantum Chem*, 2002, **90**, 1396-1403.

58. R. N. Jones, W. F. Forbes and W. A. Mueller, *Can. J. Chem.*, 1957, **35**, 504-514.
59. L. S. Crocker, G. L. Gould and D. M. Heinekey, *J. Organomet. Chem.*, 1988, **342**, 243-244.
60. A. Sylvain and C. Alain, *Statistics Surveys*, 2010, **4**, 40-79.
61. B. Srinivasan, *The FEBS Journal*, 2022, **289**, 6086-6098.
62. R.-J. van Putten, J. C. van der Waal, E. de Jong, C. B. Rasrendra, H. J. Heeres and J. G. de Vries, *Chem. Rev.*, 2013, **113**, 1499-1597.
63. M. C. Allen, A. J. Hoffman, T.-w. Liu, M. S. Webber, D. Hibbitts and T. J. Schwartz, *ACS Catalysis*, 2020, **10**, 6771-6785.